INVESTIGATING PORE SCALE CONFIGURATIONS OF TWO IMMISCIBLE FLUIDS VIA THE LEVEL SET METHOD

MAŠA PRODANOVIĆ [1], STEVEN L. BRYANT [2]

[1]Institute for Computational Engineering and Sciences, University of Texas at Austin, 1 University Station, C0200 Austin, Texas 78712
[2]Department of Petroleum and Geosystems Engineering, University of Texas at Austin, 1 University Station C0300, Austin, TX 78712 and Institute for Computational Engineering and Sciences, University of Texas at Austin

Abstract

The study of pore level displacement of immiscible fluids has scientific appeal as well as many applications, notably in oil reservoir engineering and in subsurface environmental engineering. Pore network models have been used for numerical simulation of fluid displacement over relevant physical volume sizes. An accurate description of the mechanics of displacement could significantly improve the predictions from network models of capillary pressure - saturation curves, interfacial areas and relative permeability in real porous media.

If we assume quasi-static displacement, the criteria for interface movement can be deduced from capillary pressure and local pore geometry. Several challenges arise in determining these criteria. At constant pressure and surface tension, pore scale interfaces are modeled as constant mean curvature surfaces, which are not easy to calculate. Moreover, extremely irregular geometry of natural porous media makes it difficult to evaluate surface curvature values and corresponding geometric configurations of two fluids. Finally, accounting for the topological changes of the interface, such as splitting or merging, is nontrivial.

We apply the level set method and the Surface Evolver software for tracking and propagating interfaces in order to robustly handle topological changes and to obtain geometrically correct interfaces. We describe a simple but robust model based on the level set method for determining critical curvatures for throat drainage and pore imbibition. The model is set up for pseudo-static displacements and thus simulates only the approach to spontaneous events (Haines jump, pore body imbibition). The pore scale grain boundary conditions are extracted from model porous media and from imaged geometries in real rocks.

1. INTRODUCTION

When two immiscible fluids are in contact, the interface between them supports the pressure difference (capillary pressure) $p_c = p_{nw} - p_w = 2\sigma C$ where C denotes mean

interface curvature, σ denotes surface tension and p_{nw} and p_w denote pressures in non-wetting and wetting phases respectively [Adamson and Gast, 1997]. In quasi-static displacement, we can thus model fluid-fluid interfaces as constant mean curvature surfaces. The extremely irregular geometry of natural porous media, however, makes it difficult to evaluate surface curvature values and corresponding geometric configurations of the two fluids. The analytical description of the interface (and its curvature) is known only in very specialized cases such as the capillary tube of radius r, $C = \frac{cos(\theta)}{r}$, where θ denotes the contact angle the two fluids form with the surface.

Flow simulations in the actual porous medium geometry are extremely computationally demanding, and the most common up-scaling method is simulating in a network of geometrically simplified pores (openings) and throats (constrictions). *A priori* predictions of macroscopic behavior are possible when the network is physically representative of the real medium. For instance, a dense random packing of spheres (e.g. Finney pack) is a simple model of granular media that captures some key geometric and topological features of pore space [Bryant et al., 1993, 1996]. The pore throat network of such packings is readily available via Delaunay tessellation (Fig. 1. a)).

Drainage (imbibition) simulations require a criterion for which an invading fluid occupies each throat (pore) in the network, usually in the form of the critical curvature above (below) which the throat (pore) is drained (imbibed). The first attempt to define critical curvature for imbibition was made by Haines [1930], $C_H = \frac{1}{R_{in}}$, where R_{in} is the radius of the maximal sphere inscribed into the pore body. Various empirical corrections to this formula were proposed [Jerauld and Salter, 1990; Mason and Mellor, 1995]. Jerauld and Salter, for instance, observed that a pore is more likely to be imbibed at higher curvature if it has more imbibed neighbors. Thus they proposed the critical pore imbibition curvature as $C_{JS} = \frac{C_H}{N_{NW}}$ where N_{NW} denotes the number of pores connected to the given pore which contain NW phase.

Haines also proposed that the critical curvature for drainage of a throat corresponds to a locally spherical meniscus inscribed in the throat. While Mayer-Stowe-Princen theory [Mayer and Stowe, 1965; Princen, 1969a,b, 1970] provides a rigorous alternative for 2D throats, this approach underestimates critical curvature for 3D throats [Bryant et al., 1996] and a simple extension to 3D [Johnson, 2001] does not help.

Gladkikh and Bryant [2005] implemented a dynamic, purely mechanistic set of criteria for imbibition following Melrose [1965]. The idea is topological and geometrical: when two separate menisci come into contact within the pore, they merge and the resulting instability causes the pore to imbibe. To implement this criterion, Gladkikh and Bryant [2005] idealized the interfacial surface as locally spherical in a pore throat. Imbibition proceeds by incremental decrease in curvature (equivalent to reducing pressure) and recomputation of pore level events. As illustrated in Fig. 1. b), however, simulating the topological changes of the interface, such as splitting and merging fronts, is nontrivial, even with spherical idealizations. We are, therefore, very interested in a method that liberates us from the spherical interface assumptions in order to fully utilize the known pore/throat geometry for the Melrose criterion.

Surface Evolver [Brakke, 1992] is an energy minimization approach for simulation of liquid surfaces shaped by various forces. In a porous medium imbibition simulation, at each curvature decrement the software adjusts surface vertex positions to achieve equilibrium.

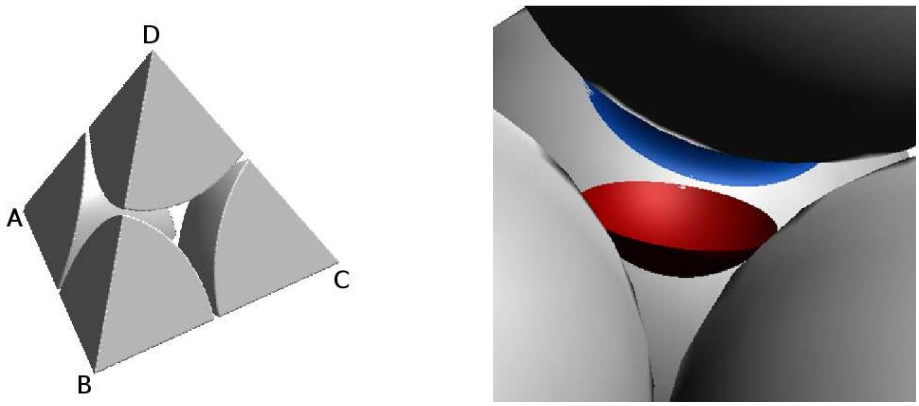

a) b)

FIGURE 1. a) A tetrahedral cell resulting from Delaunay tessellation of the Finney pack. Centers of the neighboring spheres are marked A, B, C, D. Each tetrahedral cell defines a pore body in the pack, and its sides define pore throats. b) The simplest configuration of fluids in a non-imbibed pore [Gladkikh and Bryant, 2005]. A meniscus between wetting and non-wetting phases (red) has reached a stable position (at given curvature) in the pore throat formed by lower three grains. A pendular ring of wetting phase (blue) is supported at the contact of upper and rear grains. At some smaller value of curvature the meniscus and ring will come into contact. At that moment, the two previously distinct menisci merge, become unstable and the pore will become filled with the wetting phase.

Hilden and Trumble [2003] used Surface Evolver to determine capillary pressure required to displace a liquid in a planar array of hexagonally packed spheres. Although Surface Evolver simulation of critical curvatures in pore level events (rupture and coalescence of pendular rings) in our lab [Noble and Bryant, 2002] agreed with theoretical predictions, topology changes such as the merger of three pendular rings shown in Fig. 2. have to be handled manually (e.g. the user has to remove the vertex at a pinch point).

In this paper we explore the applicability of the level set method for robust determination of critical curvatures (equivalently, pressures) for throat drainage and pore imbibition events in a wide range of microscale geometries. While some work has been done for minimal surfaces in porous media [Torres et al., 2005], to our best knowledge this is a novel application of the level set method. While the method can be used to model dynamic interface movement, we are presently concerned only with pseudo-static displacements. Thus we are interested only in asymptotic (steady-state) solutions to the level set model equation.

2. THE LEVEL SET METHOD

The level set method [Sethian, 1999; Osher and Fedkiw, 2002] was introduced by Osher and Sethian [1998] for tracking evolution of interfaces under potentially complex motions. The moving surface of interest is embedded as the zero level set of function $\phi(x,t)$, and

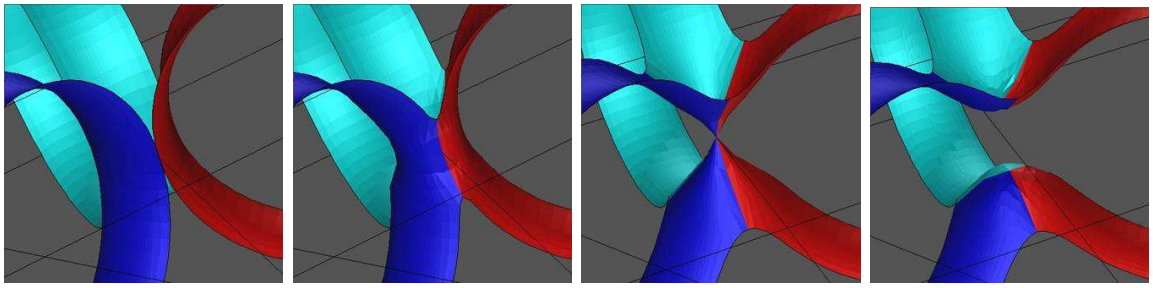

FIGURE 2. Surface Evolver simulation [Noble and Bryant, 2002] of constant curvature surfaces at decreasing values of curvature. Initial configuration (left) consists of pendular rings (in different colors) around 3 neighboring spheres (spheres not shown). With curvature gradually decreasing, wetting phase rings touch, merge, and coalesce. This sequence of events corresponds to "snap-off" of the nonwetting phase that previously occupied the pore throat between the three spheres.

the governing PDE is

$$\phi_t + F|\nabla\phi| = 0, \qquad \phi(x, t = 0) \; given \tag{1}$$

where F is the particle velocity in the direction normal to the level set. The numerical solution is built upon hyperbolic conservation laws and parabolic techniques. The method works for any dimension and handles topology changes naturally which has resulted in a vast number of applications including two-phase compressible flow, grid generation, computer vision, image restoration, minimal surfaces and surfaces of prescribed curvature.

For our two-dimensional simulations we have extensively used Toolbox of Level Set Methods [Mitchell and Templeton, 2005] which we briefly introduce here. The toolbox provides a collection of algorithms and examples (mainly from Osher and Fedkiw [2002]) implemented in Matlab for solving various forms of the level set method PDE on fixed, structured Euclidean grids. Numerical treatments of Eq. (1) provided in the toolbox are as follows: (i) Upwinding for the hyperbolic term (the first order, the second and third ENO and the fifth order WENO schemes), (ii) Central differencing for the mean curvature (parabolic) term, and (iii) Euler (the first order) or Runge-Kutta methods (orders 2, 3 and 5) for time discretization.

2.1. **Signed Distance Function Construction.** There are infinitely many level set functions that can describe a region Ω (or its boundary $\delta\Omega$) occupied by a phase of interest. Signed distance function for the interface $\delta\Omega$ at a point x is merely the distance from x to the closest point of $\delta\Omega$, with a sign reflecting whether x is inside or outside Ω. The signed distance function is a preferred level set function because of its numerical stability [Osher and Fedkiw, 2002]. Determining a signed distance function for analytically described interfaces such as spheres and cylinders is trivial. Fast Marching Method is an attractive numerical method for computation of signed distance function for an arbitrary interface [Sethian, 1999].

Even if initialized as such, ϕ will not remain a signed distance function as the interface evolves. Steepening and flattening of gradients of ϕ can introduce considerable numerical error when computing first and second order derivatives. It has been suggested to reinitialize the level set function (i.e. replace it with a signed distance function that has the same zero level set) at least periodically throughout the simulation [Merriman et al., 1994]. Reinitialization is a nontrivial effort (for an overview refer to [Osher and Fedkiw, 2002] and references therein), but we find it essential for our application.

Normal velocity F in our application is obtained from a balance of pressure and surface tension forces and is defined only at the interface. For points off the interface, however, we still use the same velocity model (and thus trivially extend the velocity field). The work of Adalsteinsson et al. [1999] describes an efficient algorithm for extension velocities which, while not necessary in our application, has been shown to preserve signed distance function property of the level set, and thus enhances accuracy.

2.2. **Prescribed Curvature Model.** The prescribed curvature level set model, $F(x,t) = \kappa_0 - \kappa(x,t)$, where κ_0 is a given constant, and $\kappa(x,t)$ is curvature of the level set function at the interface, was introduced by Chopp et al. [1993]. This model can equivalently be written in the form $F(x,t) = a_0 - b_0\kappa(x,t)$, which emphasizes the balance of pressure and surface tension forces. Surfaces of constant curvature have received relatively little attention especially compared to minimal surfaces (surfaces of zero curvature) which have direct applications in material science and computer graphics. The work of Torres et al. [2005] gives a great overview of the literature on computing minimal surfaces via the level set method.

2.3. **Slightly Compressible Model.** We propose the normal velocity F in the form

$$F(x,t) = a_0 exp[f(1 - \frac{V(t)}{V_m})] - b_0\kappa(x,t) \tag{2}$$

The first term is pressure-like with a reference pressure a_0, target volume V_m and dimensionless bulk modulus f. $V(t)$ is the non-wetting phase volume, b_0 is the surface tension, and $\kappa(x,t)$ is the mean curvature of the interface. The steady state solution of Eq. (2) is a constant curvature solution. The prescribed curvature model, while simpler, requires the initial condition surface to be very close to the steady state location for satisfactory results. In a general porous sample we know the pressure difference and the amount of fluid available, but the complex geometry does not allow us to predict the approximate position of the final interface. Our model circumvents this difficulty by allowing for interface advancement from nearly arbitrary initial position.

2.4. **Motion in Restricted Domains.** The original level set method describes the motion of interfaces that separate exactly two phases. Our application, however, involves three phases - two fluid and one stationary grain phase - and therefore triple junctions.

There has been a number of attempts to extend the method to deal with multiple phases (none of which is necessarily stationary). Aside from the computational cost of storing multiple level sets (one for each phase present) and the difficulty of defining interphase interactions, it is well known that under curvature driven motion, which is ubiquitous in applications, level sets will pull away from each other, creating a gap [Sethian, 1999]. The first scheme that tackles this problem was given by Merriman et al. [1994], followed by the

variational level set method [Zhao et al., 1996, 1998], and the projection method for the motion of triple junctions [Smith et al., 2000, 2002]. These methods can model different contact angles at triple junctions, which is of interest in modeling of wetting/non-wetting fluids in porous media.

Torres et al. [2005] studied the case where the third phase is stationary, though only in the special case of minimal surfaces. The authors use only one level set to describe the surface of interest and exploit the fact that minimal surfaces are orthogonal to the grain boundary. This approach cannot be extended to surfaces that meet the grain boundary at different contact angles. Our work presents the first application of the level set method to interfaces involving wetting/nonwetting fluids in porous media.

We account for the porous medium by imposing a constraint of the type $\phi(x,t) \leq \psi(x)$ where ψ is a fixed level set function that describes the pore space. We refer to ψ as the **mask** defining the porous medium geometry. This mask is enforced after each time integration step, as opposed to modeling the pore space boundary as a separate, stationary level set. This constraint results in a zero contact angle, although the contact angle is not specifically modeled and cannot be varied.

2.5. **Progressive Quasi-static Algorithm.** We designed a simple "progressive" algorithm for critical curvature computation.

Surface tension b_0 is set to a constant value that is used throughout simulations while pressure is increased or decreased. In **drainage simulations** we start either from the level set corresponding to plane $x = 0$ or a circular front at the same position. We then use the slightly compressible model from §2.3 to move the level set to an initial, nontrivial position. Initial pressure a_0 is set to the capillary entry pressure for the pore space opening at $x = 0$, and the simulation is run with V_m and f of choice until the steady state ϕ_I is reached. Corresponding pressure is calculated from $a_I = a_0 exp[f(1 - V/V_m)]$ where V is the volume of the non-wetting phase as described by ϕ_I.

The progressive quasi-static algorithm iteration starts from ϕ_I and pressure a_I. A step consists of an increment in curvature Δc, which we impose by increasing the pressure by $\Delta a = b_0 \Delta c$. The prescribed curvature model is then run until it reaches steady state, and the new location of the zero level set is recorded. Iteration continues until the fluid-fluid interface touches the opposite boundary of the domain. **Critical curvature** is the last curvature for which a stable configuration exists before the invading fluid occupies the entire pore space.

In **imbibition simulations** we start from an end-point of a drainage simulation and at each step run the prescribed curvature model with pressure reduced by Δa.

As a matter of practical implementation we note that increasing the surface tension value b_0 strongly affects the CFL condition, reducing the time step. In our modeling, however, only the ratio a_0/b_0 matters and b_0 can be set to a small value. Furthermore, maximal absolute error $E = max_x|\phi(x,t) - \phi(x,t-\Delta t)|$ is evaluated every $\Delta t = 0.5$ (the actual time spacing δt in the numerical discretization of Eq. (1) is independent of this value). Steady state is assumed reached when $E < E_{max}\Delta x$, where Δx is the grid spacing and E_{max} a small value, assumed 0.05 by default. The toolbox [Mitchell and Templeton, 2005] implemented a basic iterative reinitialization, which we apply to the level set after every Δt period.

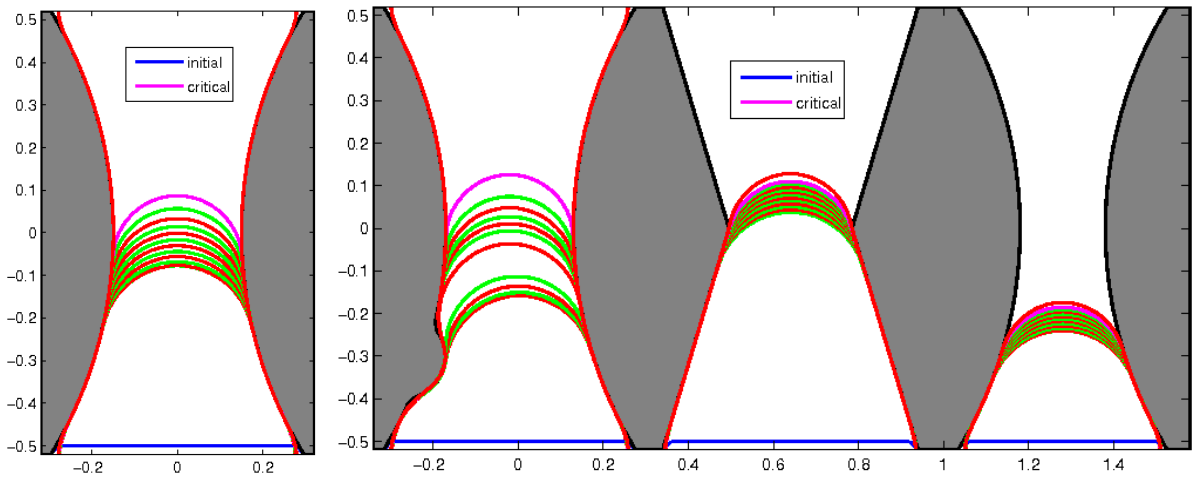

a) b)

FIGURE 3. a) A complete sequence of the progressive quasi-static algorithm for drainage in a throat delineated by spherical segments. Initial interface position is shown in blue and the subsequent steps alternate in red and green colors. The critical curvature step is in magenta color (corresponding curvature is 6.63; the exact solution is $6.6\dot{6}$). b) A sequence of the model steps for drainage in three throats in parallel. A single level set determines the interface location in all throats simultaneously. The method correctly identifies that the left-most throat drains first, at a computed critical curvature of 6.70. The menisci remain in the middle and right throats at that curvature.

3. RESULTS

3.1. **Throat Drainage.** We tested the progressive quasi-static algorithm in 2D on a number of analytically created throat geometries, with masks that are the union of signed distance functions corresponding to spherical and linear segments. Fig. 3. a) shows a complete progressive quasi-static algorithm sequence. The method's topological robustness is evident in Fig. 3. b) where the interface consists of three disjoint fronts. Furthermore, as shown on the same figure, the algorithm is robust with respect to sharp corners and "bumps" on the grain surface. Note that in both cases the computed solution has less than 1% relative error.

We further present the result in a geometry taken from a segmented X-ray image[1] of a real rock (Fig. 4.). If the mask is left in its segmented form (i.e. values of $-\Delta x$ inside the pore space and Δx outside), the low resolution and this crude mask (Fig. 4. a)) strongly degrade the accuracy. The simulated critical curvature has 7.3% relative error (the correct value is 14.91), and the position of the critical interface is not at the correct location. Magnifying the image improves the critical interface position and slightly reduces

[1]The image used here is available from the 3DMA-Rock software website at http://www.ams.sunysb.edu/~lindquis/3dma/3dma_rock/3dma_rock.html, Instructions for running 3DMA-Rock, version 12/03

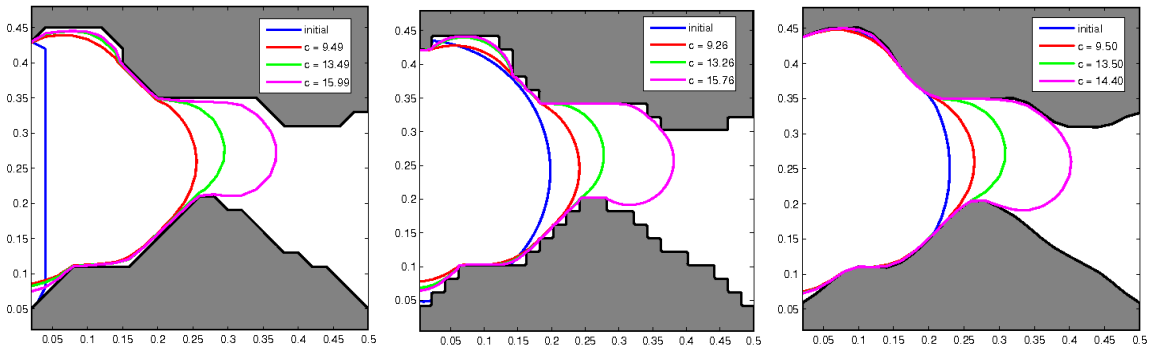

a) b) c)

FIGURE 4. Simulation in a 2D throat cut out from a slice of a segmented 3D X-ray microtomography image. Critical curvature zero level set in each plot is shown in magenta. a) Simulation with a crude mask directly from a segmented image. b) Simulation with a crude mask from the segmented image magnified 5 times (each voxel replaced by 5×5 voxels of the same value). c) Mask obtained from the segmented image as for a), but reinitialized before the simulation.

relative error (Fig. 4. b)), but this increases running time. The problem is best remedied by applying a high accuracy reinitialization routine to the mask in a narrow band around the pore-grain interface. This smooths the interface and changes the mask to a signed distance function (Fig. 4. c)), yielding a critical curvature estimate with 3.4% relative error. The reinitialization changes the underlying segmented image at a negligible number of voxels.

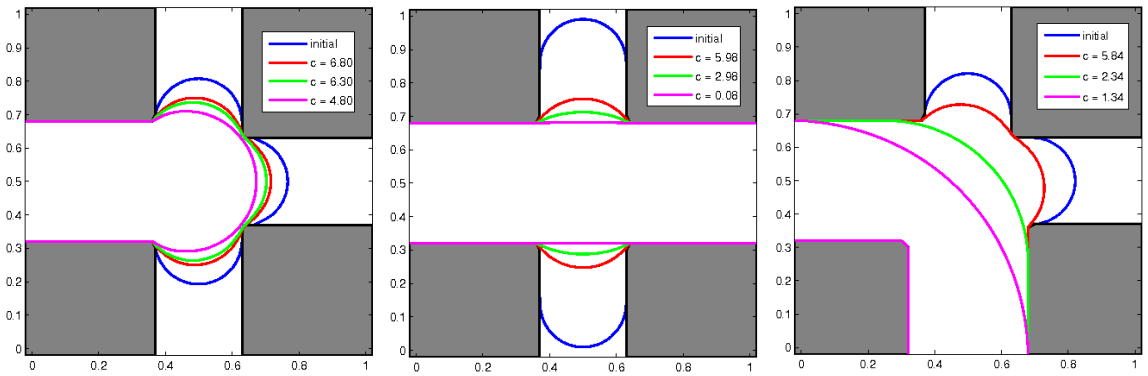

a) b) c)

FIGURE 5. Imbibition in square pores with variable combinations of attached throat channel widths. Only a few steps are shown in each figure for clarity, with the final stable stage outlined in magenta color. a) Imbibition starts from drainage curve with 3 menisci. b) Imbibition starts from drainage curve with 2 "opposite" menisci. c) Imbibition starts from drainage curve with 2 "neighboring" menisci.

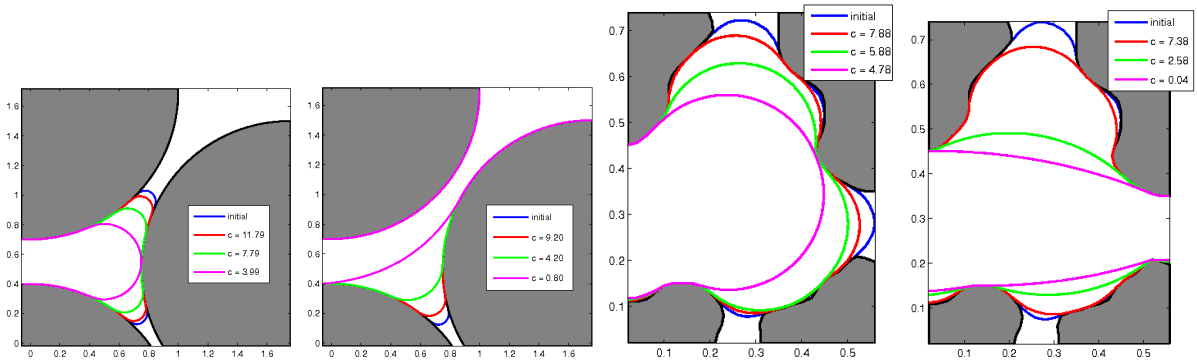

a) b) c) d)

FIGURE 6. Imbibition in two different pores. Only a few steps are outlined in each case, with the critical one shown in magenta. a) Imbibition simulation in a pore bounded by three spheres of radius 1.0. Initial step is a drainage curve with two menisci. b) Imbibition in the same pore as in a), but starting from a drainage curve with one meniscus. c) Imbibition simulation in a pore from a real geometry (same source as in Fig. 4.). Imbibition started from a drainage curve with three menisci. d) Pore geometry same as in c), however imbibition starts from a drainage curve with two (opposite) menisci.

3.2. **Pore Imbibition.** Figs. 5. a)-c) show imbibition in square pores typical for cubic network flow models. Magenta lines show the critical curvature curve (i.e. the last stable configuration before the zero level set leaves the domain). Note that if the simulation reaches zero pressure, the level set inevitably leaves the domain upon further pressure decrease, because the curvature term in the level set evolution equation is zero. Critical curvature predictions in these square pores are in agreement with those presented by Lenormand and Zarcone [1984], and Jerauld and Salter [1990]. Figs. 6. a)-b) further show imbibition in a spherical pore which are of interest in our network model [Gladkikh and Bryant, 2005]. In Fig. 6. a), the computed critical curvature of 3.99 has less than 1% relative error (correct value is 4.0). This simulation confirms the Melrose criterion: the critical curvature occurs just after the two initially distinct menisci come into contact. The method handles the change in topology automatically. Figs. 6. c)-d) show comparable results in a pore taken from a real geometry. The zero level set at curvature 0.04 in Fig. 6. d) is the last one that maintains contact with the grain boundary on the left side. Subsequent steps require information beyond the boundary, so the simulation was stopped. It is clear however that the algorithm is approaching the correct critical curvature of zero, i.e. the pore cannot imbibe when menisci are present only in "opposite" throats.

4. DISCUSSION

Preliminary simulations of pore level fluid-fluid interfaces via level set method are encouraging. The progressive quasi-static algorithm identifies critical curvatures in throat drainage and pore imbibition without manual intervention. The method is robust with respect to geometry and smoothness of pore throats and bodies. It automatically handles

the merger and splitting of multiple menisci. Furthermore, essentially the same algorithm is applicable for both drainage and imbibition simulations. In order to tackle anticipated CPU and memory problems in 3D, we are building a C/C++ code following Smith et al. [2002]. Our aim is to compute critical curvatures for individual throats and pore bodies in model porous media, then use them in a network model to predict capillary pressure - saturation curves. Finally, since the approach in the work of Smith et al. [2002] is a multiphase one, it will allow us to incorporate fluid-fluid-solid contact angle in future modeling.

5. Acknowledgements

Beth Noble carried out the Surface Evolver simulations. The authors are grateful to K. Brakke for extensive help with that work. Baker Atlas partially supported the level set development.

References

Adalsteinsson, D., and J. A. Sethian (1999), The fast construction of extension velocities in level set methods, *J. Comp. Phys.*, *148*, 2–22.

Adamson, A. W., and A. P. Gast (1997), *Physical chemistry of surfaces*, John Wiley and Sons, Inc.

Brakke, K., (1992), The Surface Evolver, *Exp. Math.*, *1*, 141–165. The software is available from http://www.susqu.edu/brakke/evolver.

Bryant, S. L., P. R. King, and D. W. Mellor (1993), Network model evaluation of permeability and spatial correlation in a real random sphere packing, *Transport Porous Media*, *11*, 53–70.

Bryant, S. L., G. Mason, and D. Mellor (1996), Quantification of spatial correlation in porous media and its effect on mercury porosimetry, *J. Colloid Interface Sci.*, *177*, 88–100.

Chopp, D., and J. A. Sethian (1993), Flow under curvature: Singularity formation, minimal surfaces, and geodesics, *Exp. Math.*, *2(4)*, 235–255.

Gladkikh, M., and S. L. Bryant (2005), Prediction of imbibition in unconsolidated granular materials, *J. Colloid Interface Sci.*, *288*, 526–539.

Haines, W. B. (1930), Studies in the physical properties of Soil 5. the hysteresis effect in capillary properties and the modes of moisture distribution, *J. Agric. Soc.*, *20*, 97–116.

Hilden, J. L., and K. P. Trumble (2003), Numerical analysis of capillarity in packed spheres: Planar hexagonal-packed spheres, *J. Colloid Interface Sci.*, *267*, 463–474.

Jerauld, G. R., and S. J. Salter (1990), The effect of pore-structure on hysteresis in relative permeability and capillary-pressure - pore-level modeling, *Transport Porous Media*, *2(2)*, 103–151.

Johnson, A. S. (2001), Pore level modeling of interfacial area in porous media, M. S. Thesis, University of Texas at Austin, Austin, TX, USA

Lenormand, R., and C. Zarcone (1984), Role of roughness and edges during imbibition in square capillaries, *Soc. Petr. Eng. J.*, no. 13264.

Mason G., and D. Mellor (1995), Simulation of drainage and imbibition in a random packing of equal spheres, *J. Colloid Interface Sci.*, *176(1)*, 214–225.

Mayer, R. P., and R. A. Stowe (1965), Mercury porosimetry-breakthrough pressure for penetration between packed spheres, *J. Colloid Interface Sci.*, *20*, 893–911.

Melrose, J. C. (1965), Wettability as related to capillary action in porous media, *Soc. Petr. Eng. J.*

Merriman, B., J. K. Bence, and S. Osher (1994), Motion of multiple junctions - a level set approach, *J. Comp. Phys.*, *112*, 334–363.

Mitchell, I. M., and J. A. Templeton (2005), *A toolbox of Hamilton-Jacobi solvers for analysis of nondeterministic continuous and hybrid systems.*, Lecture Notes in Computer Science (LNCS) 3413. Springer-Verlag, New York

Noble, B., and S. L. Bryant (2002), Using the surface evolver to model fluid in a pore space, Rice Quantum Institute 16th Annual Summer Research Colloqium, Houston, TX, USA

Osher, S., and R. Fedkiw (2002), *Level set methods and dynamic implicit surfaces*, Springer-Verlag, New York

Osher, S., and J. A. Sethian (1988), Fronts propagating with curvature dependent speed: algorithms based on Hamilton-Jacobi formulation, *J. Comp. Phys.*, *79*, 12–49.

Princen, H. M. (1969a), Capillary phenomena in assemblies of parallel cylinders I. Capillary rise between 2 cylinders, *J. Colloid Interface Sci.*, *30*, 69–75.

Princen, H. M. (1969b), Capillary phenomena in assemblies of parallel cylinders II. Capillary rise in systems with more than 2 cylinders, *J. Colloid Interface Sci.*, *30*, 359–371.

Princen, H. M. (1970), Capillary phenomena in assemblies of parallel cylinders III. Liquid columns between horizontal parallel cylinders, *J. Colloid Interface Sci.*, *34*, 171–184.

Sethian, J. A. (1999), *Level set methods and fast marching methods*, Cambridge University Press

Smith, K. A., F. Solis, and D. Chopp (2002), A projection method for motion of triple junctions by level sets, *Interfaces and Free Boundaries*, *4*, 263–276.

Smith, K. A., F. J. Solis, L. Tao, K. Thornton, and M. Olvera De La Cruz (2000), Domain growth in ternary fluids: a level set approach, *Phys. Rev. Lett.*, *84*, 91–94.

Torres, M., D. Chopp, and T. Walsh (2005), Level set methods to compute minimal surfaces in a medium with exclusions (voids), *Interfaces and Free Boundaries*, *7*, 161–185.

Zhao, H., T. Chan, B. Merriman, and S. Osher (1996), A variational level set approach to multiphase motion, *J. Comp. Phys.*, *127*, 179–195.

Zhao, H., B. Merriman, S. Osher, and L. Wang (1998), Capturing the behavior of bubbles and drops using the variational level set approach, *J. Comp. Phys.*, *143*, 495–518.